# MROI's Automated Alignment System

A.V. Shtromberg*[a], C.A. Jurgenson[a], D.F. Buscher[b],
C.A. Haniff[b], J.S. Young[b], F.G. Santoro[a], M.T. Paz[a], J.M. Steenson[a], L. Berger[a],
[a]Magdalena Ridge Observatory, New Mexico Institute of Mining and Technology, 801 Leroy Place, Socorro, NM, 87801-4681;
[b]University of Cambridge, Dept. of Physics, Cavendish Laboratory, JJ Thomson Avenue, Cambridge, CB3 OHE, UK

## ABSTRACT

The Magdalena Ridge Observatory Interferometer (MROI) will be a reconfigurable (7.5-345 meter baselines) 10 element optical/near-infrared imaging interferometer. Depending on the location of each unit telescope (UT), light can travel distances ranging from 460 to 660 meters via several reflections that redirect the beam's path through the beam relay trains, delay lines (DL), beam reducing telescope (BCR), switchyards and finally to the beam combiners (BC). All of these sub-systems comprise three major optical axes of the MROI to be coaligned on a nightly basis by the alignment system. One major obstacle in designing the automated alignment system (AAS) is the required simultaneous measurements from the visible through near-IR wavelengths. Another difficulty is making it fully automated, which has not been accomplished at other optical/near-IR interferometers. The conceptual design of this system has been completed and is currently in its preliminary design phase. Prototyping has also commenced with designs of some hardware near completion. Here is presented the current outline and progress of MROI's automated alignment system design and some results of the prototyping.

**Keywords:** Interferometer, alignment system, Magdalena Ridge Observatory

## 1. INTRODUCTION

The MROI is comprised of three major optical axes (Fig. 1) defined by the UT, the DL/BCR, and the BC axes. The DL and the BCR are considered to be on the same optical axis because there are no turning mirrors between the two systems. Depending upon the location of the UT, from start to finish, the beam will travel distances ranging from 460 to 660 meters, and undergo several direction changes via reflection. These reflections redirect the beam's path through the beam train into the delay line area (DLA) and finally into the beam combining area (BCA). *The purpose of the AAS is to provide a method for coaligning these three axes.*

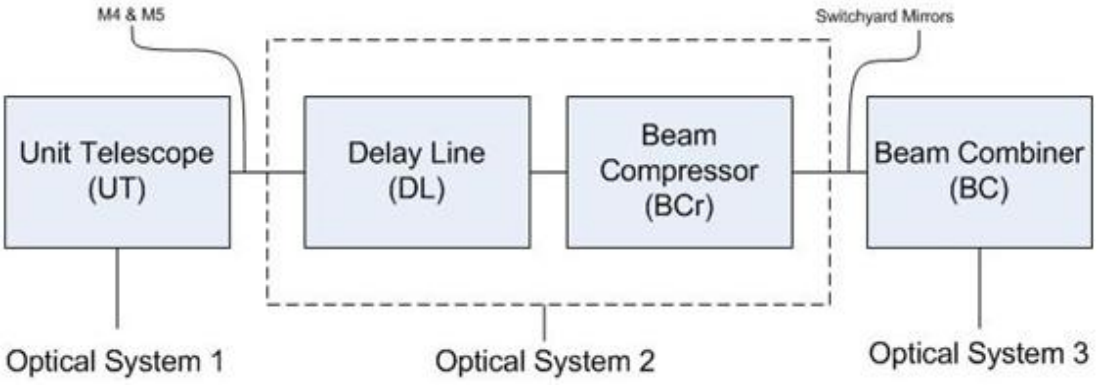


Fig. 1. Diagram showing the optical axes of the MRO Interferometer telescope.

*ashtromberg@mro.nmt.edu; phone (575) 835-5504; fax (575) 835-6807; www.mro.nmt.edu

The BCs are in the inner BCA and will be comprised of four beam combining tables that will simultaneously operate at visible through IR wavelengths, with one undetermined visitor instrument table. The first table will be for visible science, the second table will be for IR science, and the third table will be for IR fringe tracking. Each combiner has its own "switchyard," which will consist of a pair of optics to select a given bandpass, and send it to the appropriate combiner (Fig. 2). Table 1 shows the operating wavelengths for each combiner. Note that the current design omits alignment discussions on the visiting instrument and its switchyard. However it is assumed that the AAS will be able to accommodate this BC if necessary with minimal upgrade.

Table 1. Table showing the operating wavelengths and the corresponding beam combiners for the interferometer.

| Wavelength, $\lambda$, ($\mu m$) | Bandpass | Beam Combiner |
|---|---|---|
| 0.656, 0.650-1.0 | $H_\alpha$ | Visible |
| 1.1 – 1.39 | J | IR Science |
| 1.5 – 1.8 | H | IR Science, FT |
| 2.0 – 2.4 | K | IR Science |
| 1.99 – 2.31 | $K_s$ | FT |

Figure 2 shows a general optical layout of one of the telescopes and its beam path from the UT to the BCs. Upon exiting the UT, a 95mm beam enters the beam relay (in vacuum), gets directed into the DLA and finally exits into the BCA. It then gets compressed (7.308x) to a 13 mm diameter beam by a beam compressing telescope (BCR) before encountering the switchyard and the beam combining table[1].

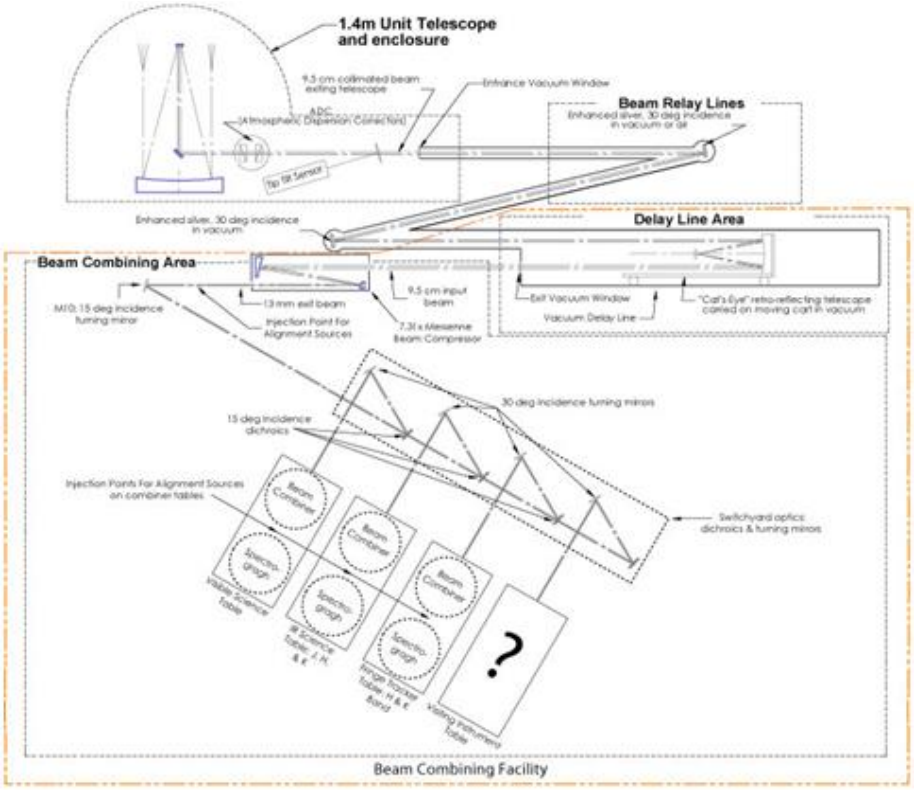

Fig. 2. Optical layout of beam path from UT to BCA.

Figure 3 is a ray trace that highlights the 6 optical assemblies that make up a single beam train of the interferometer to the first switchyard. Note that the beam path proceeding downstream starts at the UT and goes through the beam relay, then to the cats-eye (DL), the BCR, a turning mirror M10, the switchyard, and finally the BC.

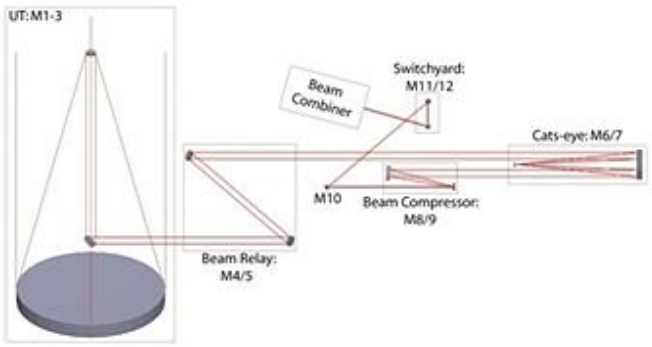


Fig. 3. Abbreviated optical train for a UT on the west arm of the interferometer to the first SY. Note the 6 optical assemblies.

Table 2 lists the names, location, and shape of the optical components. The highlighted rows indicate the pairs of mirrors that will be used by the AAS to make alignment corrections.

Table 2. Names of mirrors and their component names, locations and shapes. The highlighted rows indicate the mirrors (pairs) that will be used by the AAS to make alignment corrections.

| MROI Name | Component Name | Location | Shape |
|---|---|---|---|
| M1 | UT Primary | UT Structure | Parabolic |
| M2 | UT Secondary | UT Structure | Parabolic |
| M3 | UT Tertiary | UT Structure | Flat |
| M4 | Beam Relay Flat 1 | Beam Relay | Flat |
| M5 | Beam Relay Flat 2 | Beam Relay | Flat |
| M6 | Cats-Eye Primary | DL Cart | Parabolic |
| M7 | Cats-Eye Secondary | DL Cart | Flat |
| M8 | Beam Reducer Primary | BCA | Off Axis Parabolic |
| M9 | Beam Reducer Secondary | BCA | Off Axis Parabolic |
| M10 | BC Turning Mirror | BCA | Flat |
| M11(VIS/FT/IR) thru M16 | Switchyard Components | BCA | Dichroics & Flats |

Table 2 is important because it highlights that a pair of mirrors are needed to remove the tilt and shear between optical axes. Figure 4 shows the hypothetical situation of a beam that has both tilt and shear errors[2]. In the diagram the "red ray represents the path of an alignment laser that has been back propagated, and the black line represents the ideal path that the ray would take if the mirrors, M1 and M2, were properly aligned. Following M1 would be a detector system capable of measuring beam shear and tilt, and it is assumed that the light arriving at M2 travels along the ideal axis. In the diagram on the left, M2 is adjusted to remove the beam shear at M1. In the middle diagram, M1 is adjusted to remove tilt, and the right shows the beam coaligned with the ideal axis."[2]

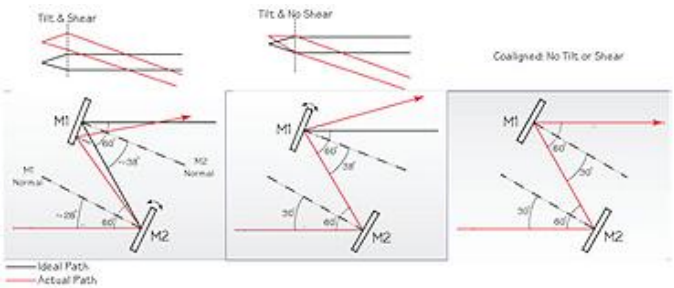


Fig. 4. A ray trace diagram showing two situations: the red line represents a misaligned beam path in tilt and shear for the two misaligned mirrors. A black line represents the ideal path of the beam with no tilt and shear errors once the mirrors have been adjusted.

It should also be noted that the *automated* alignment system refers to the alignment of the interferometer prior to observations on a nightly basis. The initial aligning of the fiducials will not be automated and will require human presence at the appropriate locations (however fine alignment of the fiducials, specifically actuation of the beamsplitters (see Sec. 2.1) will be automated and part of the automated alignment system). This is referred to as the "internal alignment" of the AAS. It is (although not yet precisely known) expected to be done on a time scale of weeks. The AAS is not responsible for the internal alignments of four optical assemblies containing curved optics (i.e. UT, DL, BCR, and BC) nor is it responsible for the initial alignment of the whole interferometer.

# 2. AUTOMATED ALIGNMENT SYSTEM HARDWARE DESIGN

## 2.1 Primary Fiducial

The purpose of the primary fiducial is to establish a reference axis, in this case the DL/BCR axis, to which the UT and BC axes must be coaligned. The primary fiducial is situated on the alignment table, located in the inner BCA immediately following the BCRs (Fig. 5).

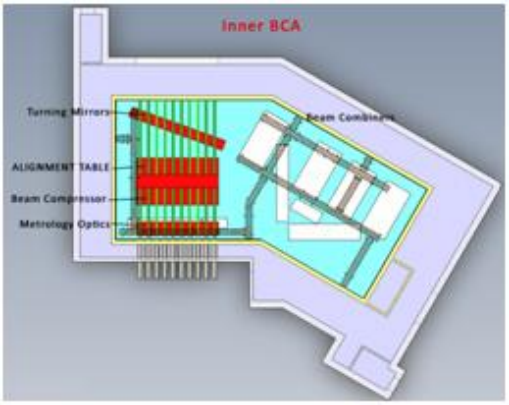


Fig. 5. Alignment table location in the inner BCA with respect to the other tables surrounding it.

Figure 6 shows a general layout of the alignment bench. The primary fiducial will consist of two light sources whose beam paths are directed toward a series of beamsplitters on slides that result in beams being sent in two different directions. An LED source (635nm), travelling upstream to the UTs and a white light source, travelling downstream to the BCs, will be located on one end of the table. A collimating setup dubbed the Magic Optical Box (MOB) at one end of the alignment table includes the light sources and ensures that both beams are collimated, stopped down to the same diameter, and follow the same optical path. There are as many beamsplitters on slides as UTs, so for 6 UTs there will be 6 beamsplitters. A corner cube Retroreflector (CCR) is located opposite the MOB, and reflects the beam back to the beamsplitters so that the beam travels in opposite directions (toward the UT and BCs).

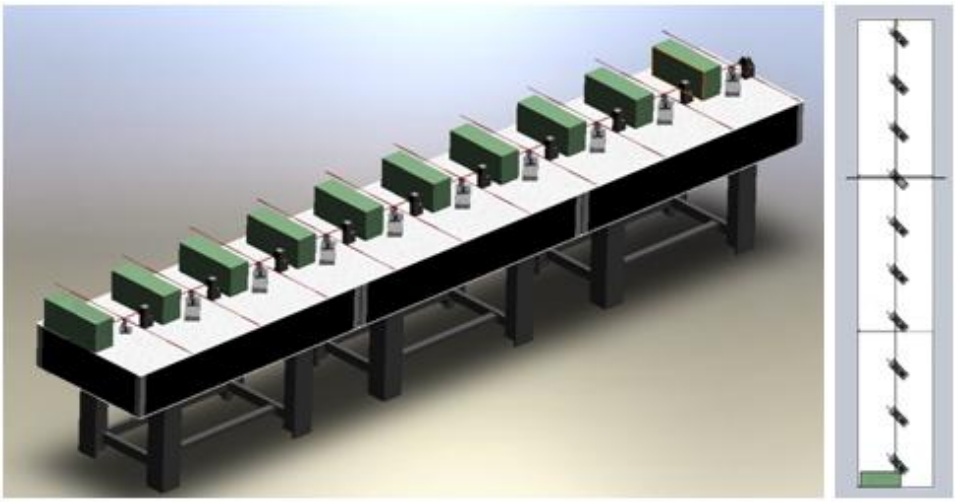

Fig. 6. General layout of optical and opto-mechanical components of the primary fiducial on the alignment table. The green box is the magic optical box (MOB) that consists of the two light sources and collimating components. On the other side of the beamsplitter is a CCR that returns the beam to the beamsplitters which will reflect it to the BCs.

The beamsplitters are located in the optical path with a 45° angle of incidence, are 1" in diameter, and have coatings (front coat, anti-reflection coat on back—with 50:50 reflection/transmission ratio) that operate from visible to NIR wavelengths. The beamsplitters will be mounted into a custom made mount (Fig.7) which will be placed onto a slide.

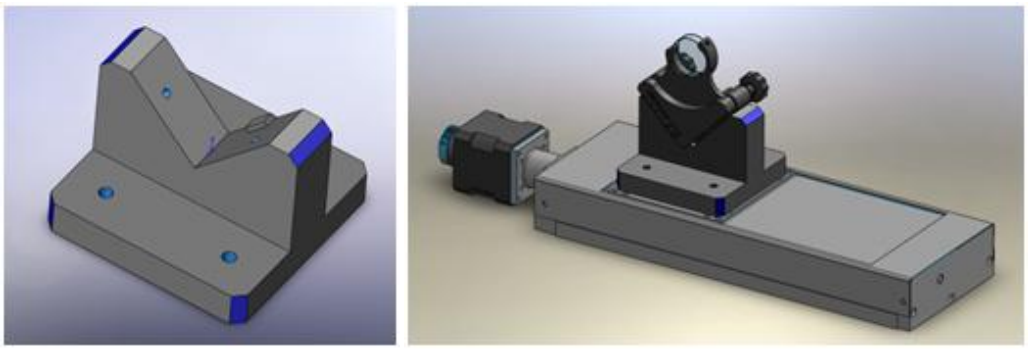

Fig. 7. A custom base mount design for the beamsplitter optic-mount assembly (left). A full beamsplitter opto-mechanical assembly located on the alignment bench (right).

It is important to discuss alignment of the beamsplitters further because of the optical phenomenon that is associated with them being plates. Figure 8 is a diagram of a plate beamsplitter showing the path a beam would follow from either of the light sources. When the beamsplitter is inserted into the optical path of the beam, a portion of the beam will be reflected 90°, and a portion of it will be transmitted with a slight displacement due to refraction. This displacement must be accounted for because when the CCR reflects the beam back to the beamsplitter, it does not arrive at the same location as the input beam. The result is that the beam traveling to the UT is not collinear with respect to that traveling to the BCs. Therefore, to ensure that the reflected portion is on the same optical axis as the original reflected beam, the CCR must be displaced appropriately. This displacement must be accounted for as precision alignment of the beams will be necessary to minimize primary fiducial errors.

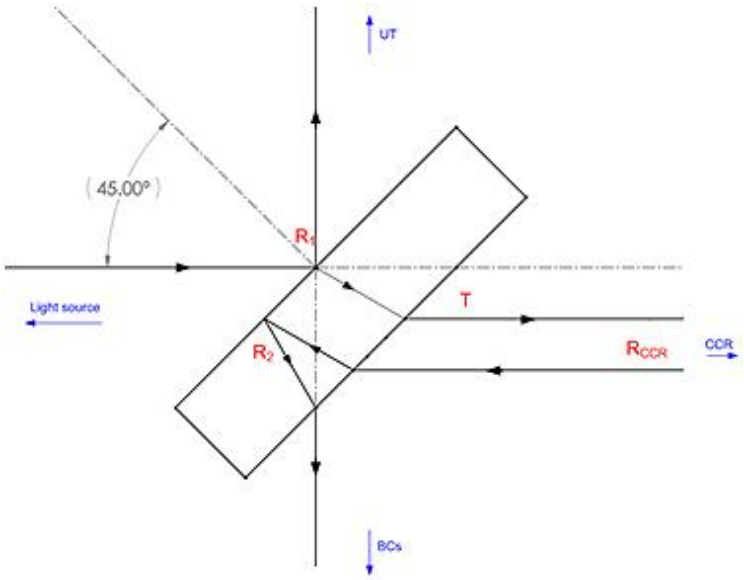


Fig. 8. A diagram of a plate beamsplitter showing reflected and transmitted of an incoming beam of light. The original reflected beam, R1 and the reflected beam R2 (post CCR reflection) must be on the same optical axis.

Figure 9 shows a top view of the MOB. Figure 10 shows the MOB from three different angles. The MOB consists of a covered "box" (shown in Fig. 6). It has a rectangular base machined for precision optical and mechanical component placement and alignment that will sit on top of the alignment bench. The two light sources are to the left of a wall block. A pin hole is placed in the wall block at the focus of a light collecting optic. On the other side of the wall block is an off-axis parabola (OAP) which functions as a collimator. An iris located on the outside wall of the MOB cover will allow the beam to be stopped down to a desired diameter. In the default state, the LED beam gets directed upstream, and is used to align the DL/BCR axis to the UT axis. The white light source is used to align the DL/BCR axis to the BC axis.

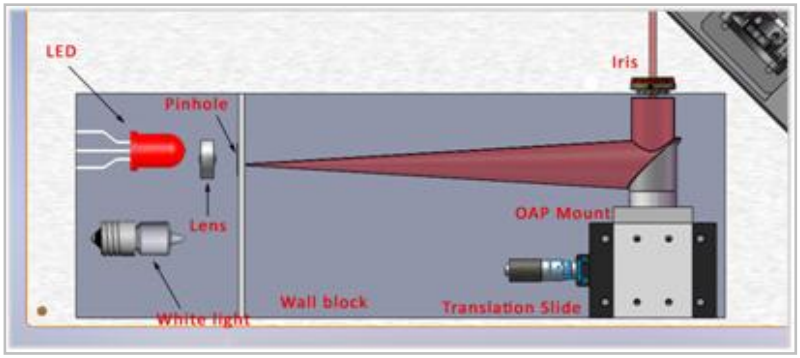


Fig. 9. Top view of the MOB. The MOB consists of two light sources (LED and a white light); a wall to block all light except the light entering the pinhole; an off-axis parabola (OAP) is mounted on a focusing translation slide which collimates the light; an iris stops the collimated beam down to a desired diameter. (Note location/placement of the light sources is not depicted accurately.)

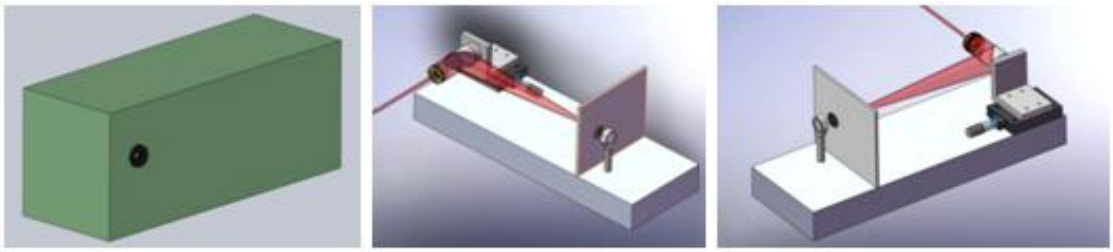

Fig. 10. Views from several angles of the MOB. Note that light source are not shown.

### 2.2 Tilt and Shear Correction/Measurement at the UT

Detection and measurement of tilt and shear errors between the UT and the DL/BCR optical axes will take place on the UT Nasmyth Table. A pair of turning mirrors, specifically M4 and M5 in the beam relay, will be used to remove those errors. Tilt and shear must be measured differently and therefore cannot be done at the same time. When measurement and alignment is taking place, shear measurement and shear correction will take place first. When the shear error between the two axes is determined M5 can be used to make the appropriate correction. After shear correction is completed, tilt measurement can begin. Once the angular displacement of the spots on the detectors is determined, then tilt error can be corrected by moving M4. Note that moving M4 and M5 must be an iterative process because moving one mirror (e.g. for tilt) will affect both tilt and shear. Therefore making the corrections for tilt and shear will probably occur after measurement of both errors. The methods of measuring tilt and shear errors between the two axes vary in their complexity, and must be explained carefully.

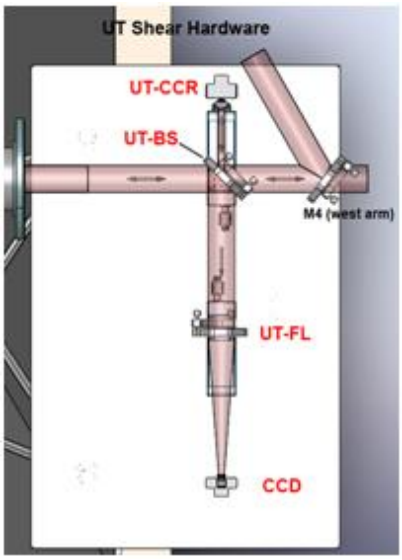


Fig. 11. A top view of the Nasmyth Table showing only the shear measurement hardware.

Measuring the shear error between the UT optical axis and DL/BCR axis, requires reimaging the telescope pupil. To do this, a ring of 4 equally spaced LEDs located around the primary will illuminate M2. The LED beam is entering the Nasmyth Table from the left where it is reflected by the UT-BS to the focusing lens which re-images the UT pupil onto the CCD. To measure the location of the DL/BCR axis the primary fiducial LED beam enters the Nasmyth Table from the right where it is reflected at the UT-BS to the UT-CCR which reflects the beam toward the UT-FL which images the beam the same distance away as the UT pupil (approximately 8.5 meters away from the CCD). The displacement between the two spots on the CCD is then corrected for by M5. Figure 12 is a diagram of the configuration being presented and shows important information regarding the positions of the various optical elements in this set-up.

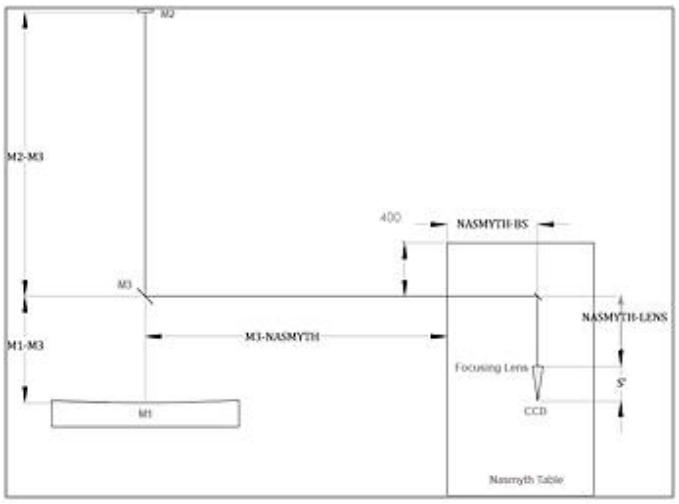


Fig. 12. A diagram of the optical path to re-image the UT pupil. Four LEDs located around M1 illuminate M2 where it is reflected toward the Nasmyth Table via M3. A beamsplitter diverts the LED light to the focusing lens which images the four spots onto a CCD. The center location of the four LEDs is used to calculate the centroid.

Tilt measurements are made with the fast tip/tilt (FTT) system[3] camera. In this case, the UT LEDs are not required to represent the UT axis. Rather M3 is put into retro-reflection mode where it reflects the primary fiducial beam. Upon arriving at the Nasmyth Table, a portion of the primary fiducial light is split off by the tip/tilt dichroic which directs the beam to the FTT CCD (via a CCR that is located below the FTT and the focusing OAP); this spot represents the DL/BCR axis. A portion of the beam is then transmitted to, and reflected by M3 to the FTT CCD. The outer axis of the UT is then rotated to see if there is relative motion of the spot from M3's reflected light with respect to the spot that represents the DL/BCR axis. This relative motion is representative of tilt, or angular error between the two axes. M4 is adjusted to correct for this.

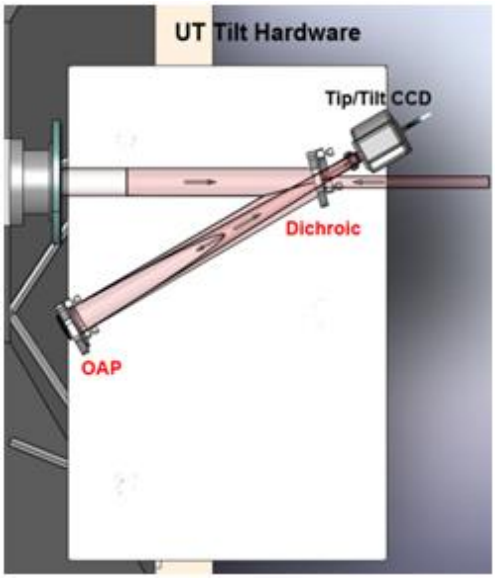


Fig. 13. UT tilt measurement hardware utilizes the hardware for the FTT system.

Figure 14 shows all the AAS components on the Nasmyth Table.

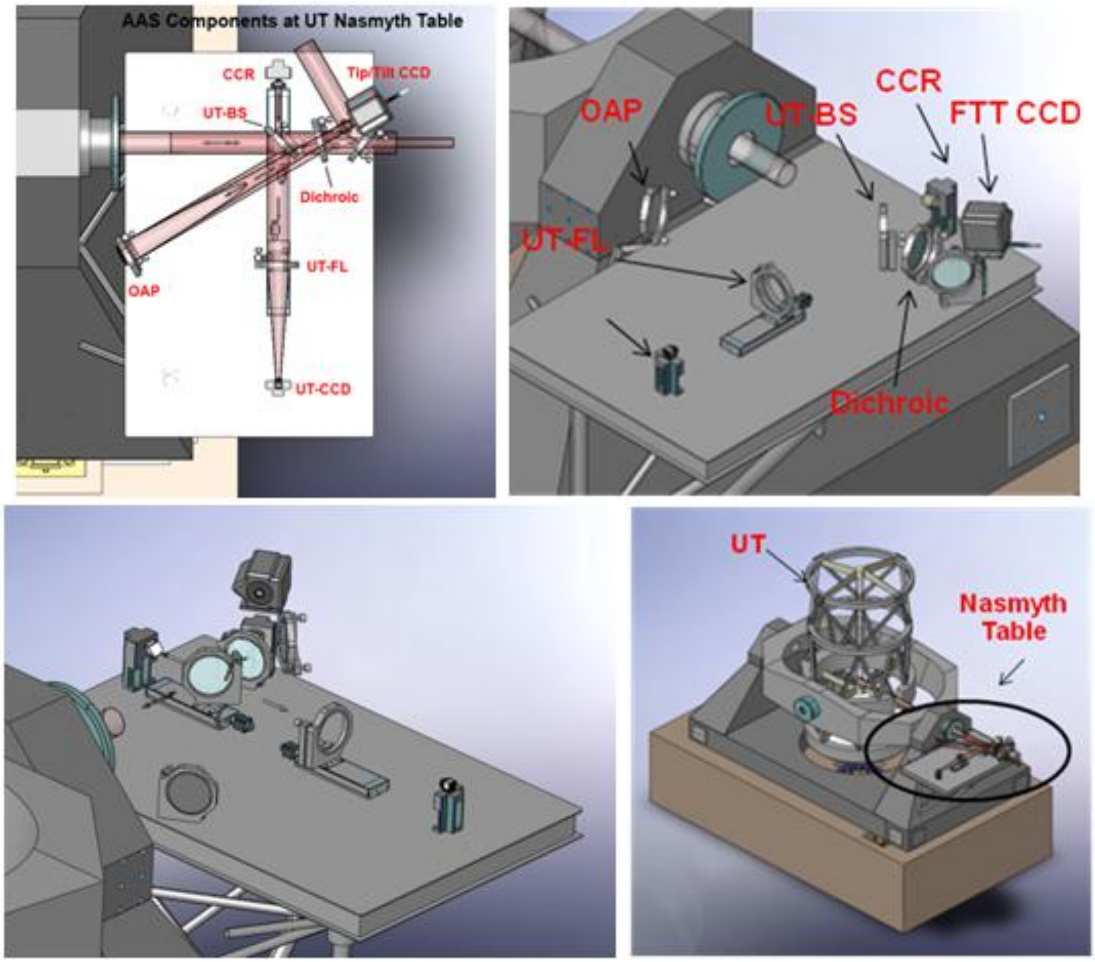


Fig. 14. All AAS components on the Nasmyth Table. The UT-BS slides in the path of the beam when tilt and shear measurements are taken. The UT-CCD is used for shear measurements. The FTT CCD is used for tilt measurements.

### 2.3 Tilt and Shear Corrections/Measurements at the Fringe Tracker BC

The interferometer's beam combiners will consist of four separate instruments: the visible science BC, the IR science BC, and the fringe tracker (FT) BC. All three instruments will have their own optical axis to which the DL/BCR axis is aligned to. Currently no design plans exist for the visible science BC. The IR science BC design is currently in the conceptual phase, but not defined in enough detail to be discussed. Therefore only the alignment mechanism for the FT BC is discussed here.

Similar to the Nasmyth Table design, the beams at the fringe tracker table are diverted from their path to tilt and shear detectors. The fringe tracker beam combiner is designed so that it combines "light from nearest neighbor telescopes"[4], so for 10 telescopes (i.e. 10 beams at the combiner input) there are 9 combined output beams. There will be a total of 9 ("flipper") mirrors located at the 1st set of combiner outputs (see Fig. 15) which will divert the beams toward the beamsplitter. The beamsplitter reflects a portion of the beam to a 2-6x variable beam reducer for shear measurements and transmits the other portion of the beam to an OAP for tilt measurements. The beam compressing optical assembly is necessary to reduce the size of the beam to accommodate the detector array size. Figure 15 is a 2-D schematic of the Fringe Tracker BC highlighting all the combination partner output beam locations for the given individual input locations.

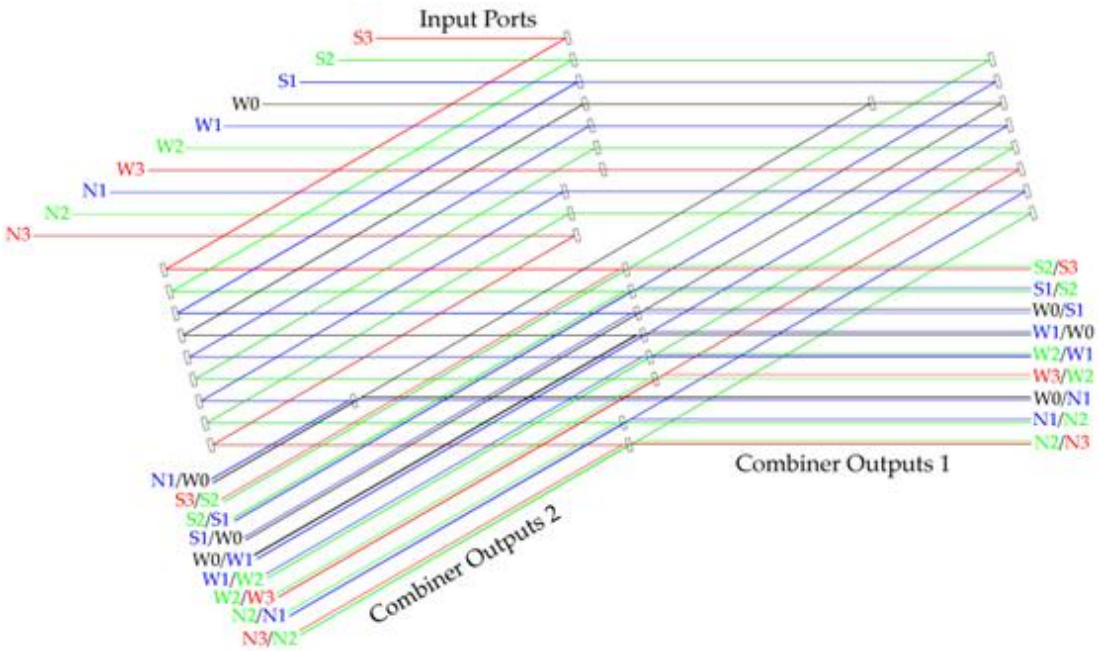


Fig. 15. Fringe Tracker BC 2D schematics showing the two BC outputs. Tilt and shear detection will only place only at Combiner Output 1.

In order to align this combiner axis to the DL/BCR axis, the white light source is directed toward the FT switchyard and then on to the combiner tilt and shear detectors. The BC axis is not defined by its own light source. Rather, relative tilt and shear measurements are made in the combination plane between combination partners. The beam that corresponds to the vertex telescope (W0) is propagated from the DL/BCR to the BC, and is used as the reference to correct for tilt and shear errors between its adjacent telescopes (i.e. all the 1—or inner—telescopes). Once aligned, the inner telescopes then will be used as a reference for the next adjacent telescopes (i.e. all the 2—middle--telescopes). When the middle telescopes are aligned, then all the outer telescopes are aligned to the middle telescopes. The optics located on the FT BC table will serve the purpose of directing the primary fiducial beams to a pair of detectors located on the FT BC table. Figure 15 shows a close up view of the optical layout for the AAS components on the table.

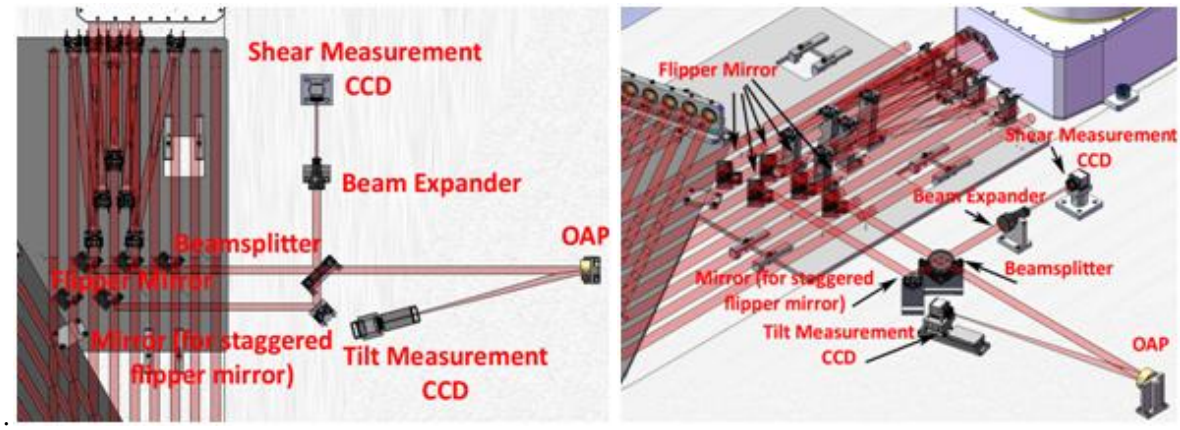


Fig. 16. A close up view of the optical assemblies involving AAS on the Fringe Tracker BC table.

Figure 17 is a 3D view of the FT BC with one of the beam outputs redirected toward the AAS components for the tilt and shear cameras.

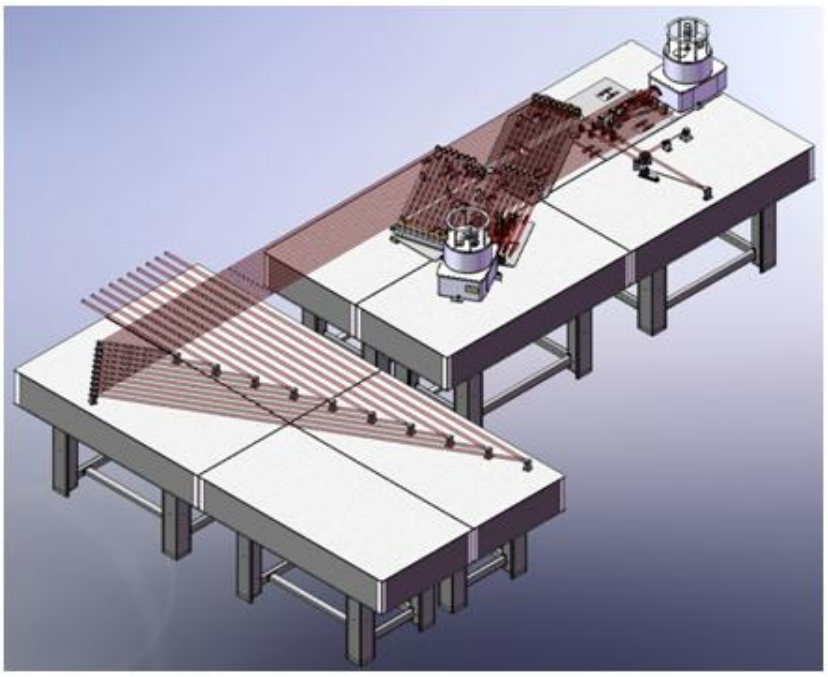

Fig. 17. FT BC 3D schematic showing all BC outputs being directed to the tilt and shear cameras.

Finally, the amount of light that will get through to the detectors is also expected to be considerably smaller than the initial beam intensity. Given that the availability of off the shelf detectors cuts off at H-Band, alignment for the fringe tracker and IR science combiners must be done in this bandpass. Therefore the white light beam must pass through the SY optics, and when the H-Band dichroic is in place in the IR science combiner switchyard, it is being assumed that ~1% of it will bleed through to the FT BC. This means that throughput to the tilt detectors can vary from ~0.034% to 3.4% and the throughput for the shear detectors will vary from ~0.029% to 2.9% depending if the IR Science Combiner is observing in H or K bands.

### 2.4 Secondary Fiducial – Quad Cells

NPOI type quad cells[5] will be used as secondary fiducials to look at the shear of the beam as it travels upstream through the beam relay, to the Nasmyth Table. The quad cells will be located starting at the exit of the DL in the BCA, inside the vacant vacuum cans at the array arm junctions and also in front of M4. Figure 18 illustrates the dimensions of the compact quad cell.

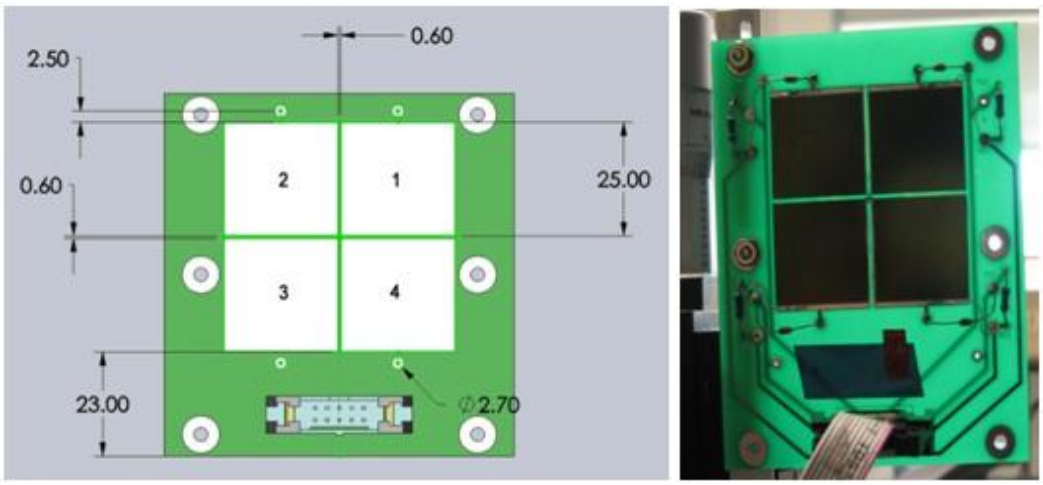


Fig. 18. Small pop-up quad cell. The design of the quad cell is the same with the exception of its dimensions (left) and the fact that it will be attached to a pop-up device (not shown). A quad cell prototype has been built and tested in a lab (right).

The quad cells consist of 4 independent space qualified, silicon solar cells. Mounting of the cells onto the background circuit board must be done precisely in order to achieve accurate centroiding. Conductive copper pads will be etched onto the circuit board to which the solar cells will be soldered. For the 4 independent solar cells, each individual cell will have to be tested to determine their voltage output levels. To improve stability, the design of the quad cells will be simple and symmetric with a minimum amount of hardware elements. This approach will result in a small form-factor and simple construction since real-estate and cost is limited. Each cell will be matched up with three others of similar performance. If 4 cells cannot be matched then they will have to be calibrated with respect to one another in the software. The cells will be configured to present analog voltage signals to a commercially available connector and ribbon cable. The analog signal may be filtered and/or amplified, then digitized by an analog to digital converter to be read into a computer.

The data acquisition instrument will read the outputs from the cells and measure the position of the beam relative to the center of the device given by

$$x = \frac{(c_1 + c_4) - (c_2 + c_3)}{c_1 + c_2 + c_3 + c_4} \qquad y = \frac{(c_1 + c_2) - (c_3 + c_4)}{c_1 + c_2 + c_3 + c_4} \tag{1}$$

where the cells are numbered counter-clockwise from the upper right.

## 3. PROTOTYPING

Currently the small quad cells have been prototyped (see Fig. 18) in the laboratory. Figure 19 shows plots of preliminary test results showing the voltage trend of a laser beam moving across the quad cell in the *x* direction (a) and in the *y* direction (b). The 4 different lines represent each solar cell voltage output. From these initial tests it can be concluded that the solar cells behave similarly, but not exactly the same, therefore in depth characterization of the cells will be necessary so that accurate software calibration can be achieved. Repeating these tests at small increment movements also show that the quad cells can detect displacements at the 25µm level. Repeatability has yet to be determined.

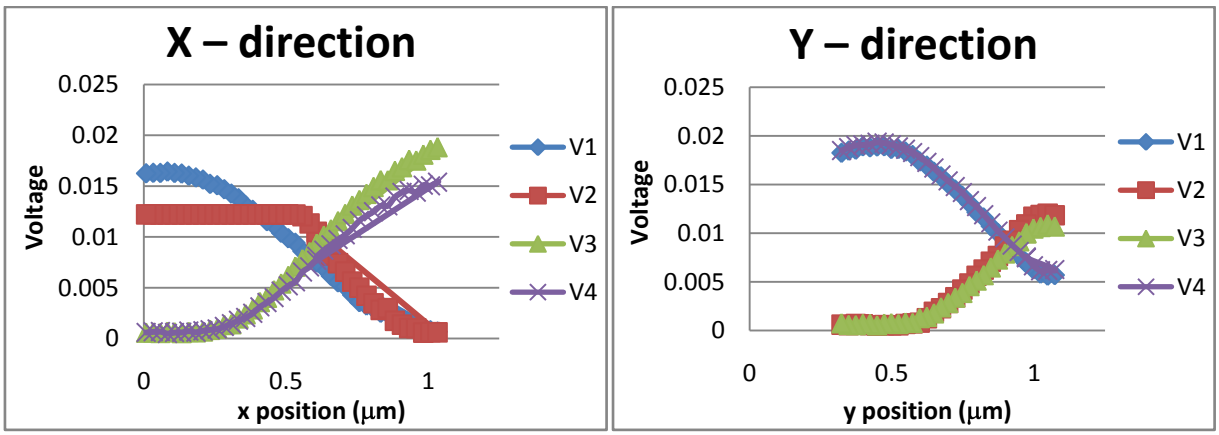


Fig. 19. Plots of voltage outputs from each solar cell on the quad cell prototype for x direction (side to side) movement (left) and y direction (up/down) movement. At any point two cells were gaining more light while the other two were losing light, hence voltage.

## 4. AUTOMATED ALIGNMENT SYSTEM ENGINE – "THE BRAIN"

The AAS has several primary functions which include the following:

- Perform the alignment procedure in an appropriate set sequence
- Receive raw data from detectors → perform centroiding calculations → determine centroiding errors
- Feed appropriate offset values to M4/M5 and to SY optics for tilt/shear corrections → recheck alignment again by receiving raw data from detectors → perform centroiding calculations to confirm alignment
- A Mode to perform "quick checks" using pop-up quad cells

- Pass data to the archiving system
- Pass data to the user interface

The AAS Engine will perform these tasks and procedures remotely, that is, all the tasks of the AAS which include initiation of the system, measurements, and corrections must be achieved from the control center i.e. user interface. This will be done in a fully automated fashion, that is when the AAS is set to run the alignment, it does the whole sequence of alignment without the need for interference from the user. This of course does not deter from the need of having manual mode since troubleshooting will be inevitable.

## 5. CURRENT STATUS

The AAS has completed its conceptual design review with great success and is currently in its preliminary design phase. A review/completion is expected in October of 2008. A final design review is scheduled for early 2009. Prototyping of the Fringe Tracker BC AAS components will commence in August of this year with expected completion by the preliminary design. This includes prototyping and testing of all hardware and the software necessary to utilize the hardware. The portion of the software that will be completed will include centroiding algorithms, controlling slides, tip/tilt actuation, and flipping mirrors. Centroiding, slide and tip/tilt control software can also be used for the Nasmyth Table and Primary Fiducial table CCDs, slides, and actuators as well.

Post preliminary design review, prototyping on the UT Nasmyth table components will begin. With its completion the Primary fiducial will then be assembled in the lab. The software portion will continue its development in parallel with the hardware prototyping. It will be impossible to assemble all the AAS hardware in a laboratory environment; therefore it will be assembled on site during site acceptance tests in summer of 2010.

## 6. ACKNOWLEDGEMENTS

A very special thank you to Dr. Daniel H. Lopez, President of New Mexico Institute of Mining & Technology and to Dr. Dave Westpfahl, Physics Department (New Mexico Tech) Chair for their support to go to the SPIE 2008 conference in Marseille, France. Also a special thanks to SPIE for their support.

The Magdalena Ridge Observatory (MRO) is funded by Agreement No. N00173-01-2-C902 with the Naval Research Laboratory (NRL). MRO Interferometer is hosted by the New Mexico Institute of Mining and Technology (NMT) at Socorro, NM, USA, in collaboration with the University of Cambridge (UK).

## REFERENCES

[1] M. Creech-Eakman et. al, "Magdalena Ridge Observatory Interferometer: progress toward first light," Proc. SPIE 7013 (2008).

[2] C. A. Jurgenson, D. F. Buscher, M. J. Creech-Eakman, C. A. Haniff, J. S. Young, T. A. Coleman, C. B. Parameswariah, E. Seneta, and E. J. Bakker, "MROI's automated alignment system," Proc. SPIE 6268, 62683Y (2006).

[3] R. Selena, "Conceptual design for the fast tip-tilt system for the MRO Interferometer," Internal document, (2007).

[4] C. A. Jurgenson, "Fringe tracker preliminary design," Internal document, (2007).

[5] G. Charmaine Gilbreath & D. Mozurkewich, "Large Aperture Quad Cell for Fiducial Alignment with Large Diameter Beams," SPIE, 4006, 1128, (2000).